Electronic Supplementary Material (ESI) for Journal of Materials Chemistry A.
This journal is © The Royal Society of Chemistry 2023

# Supporting Information

## Stable Perovskite Photocathodes for Efficient Hydrogen Evolution in Acidic and Basic Conditions.

Saikiran Khamgaonkar[a], Qiaoyun Chen[b], Kevin Musselman[b] and Vivek Maheshwari *[a]

[a] Department of Chemistry, Waterloo Institute for Nanotechnology, 200 University Ave. West Waterloo, ON N2L 3G1, Canada

[b] Department of Mechanical and Mechatronics Engineering, University of Waterloo , University Ave. West, Waterloo, ON N2L 3G1, Canada

E-mail: vmaheshw@uwaterloo.ca

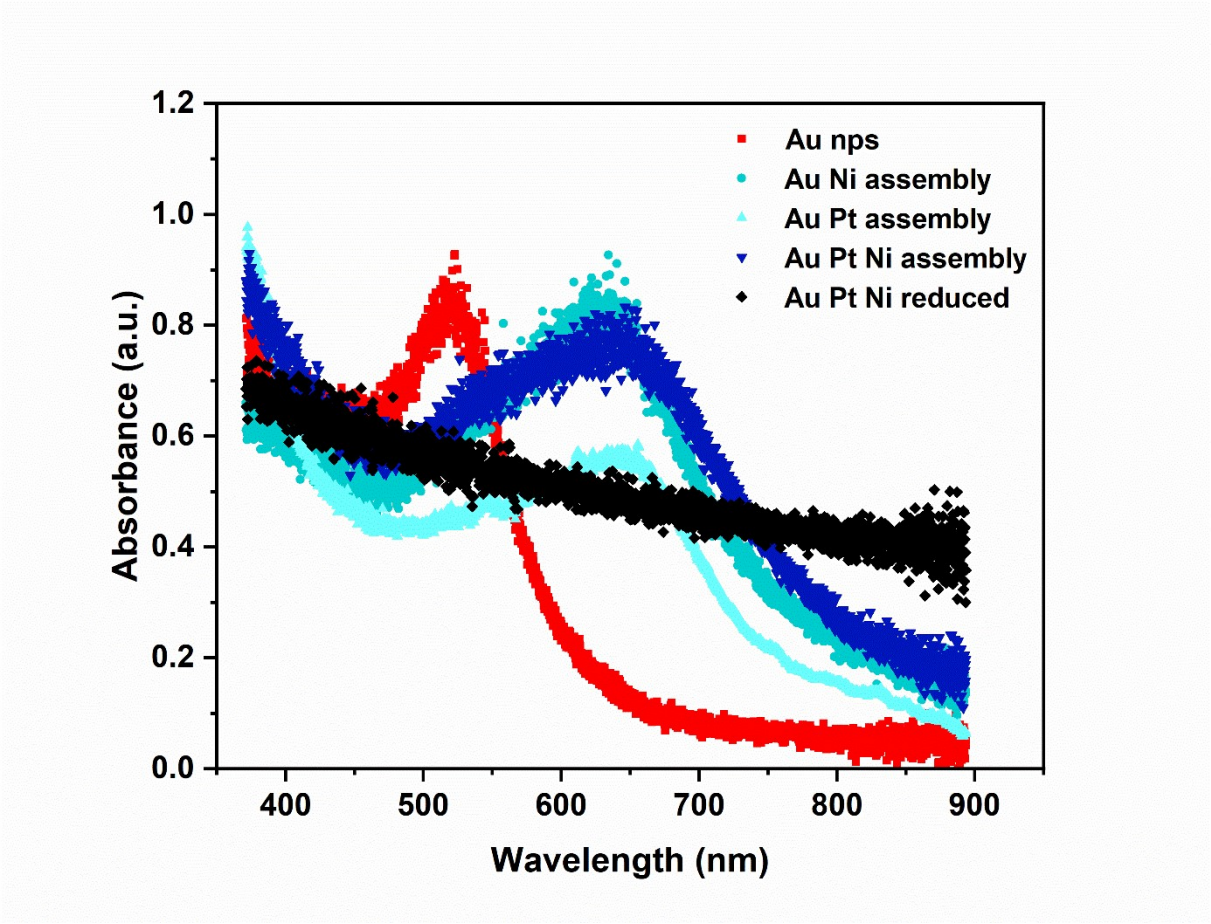


**Figure S1** UV visible absorbance spectrum of Au nanoparticles, Au-Ni, Au-Pt -Ni, Au-Pt-Ni reduced chains.

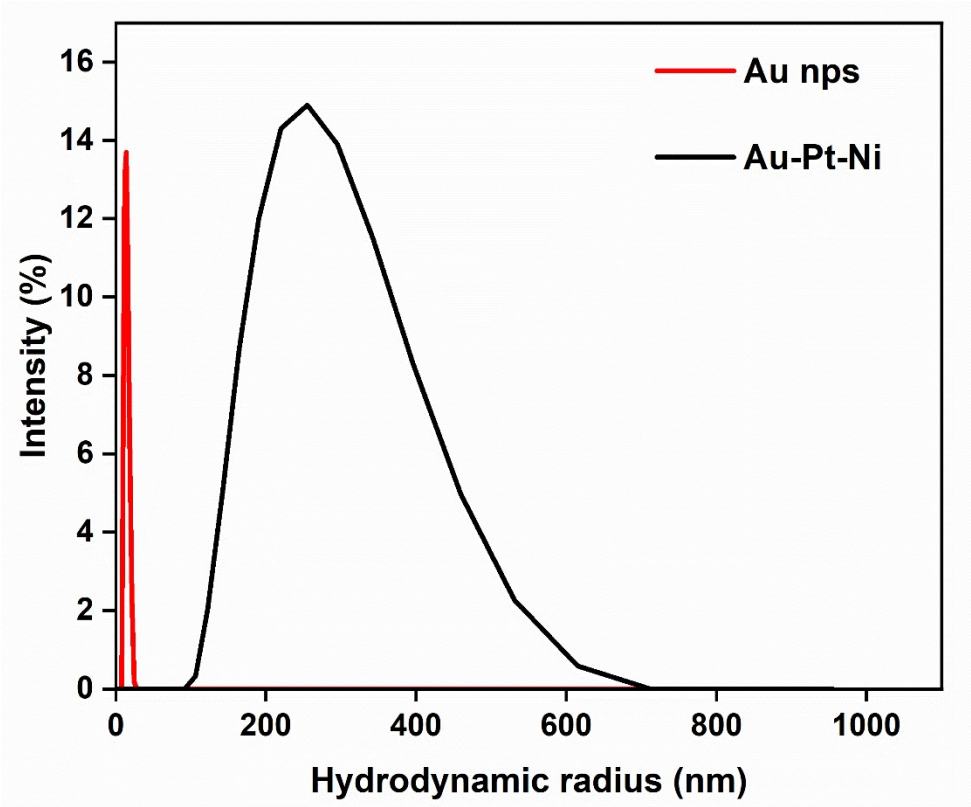


**Figure S2** Dynamic light scattering results of self-assembly of Au-Pt-Ni chains.

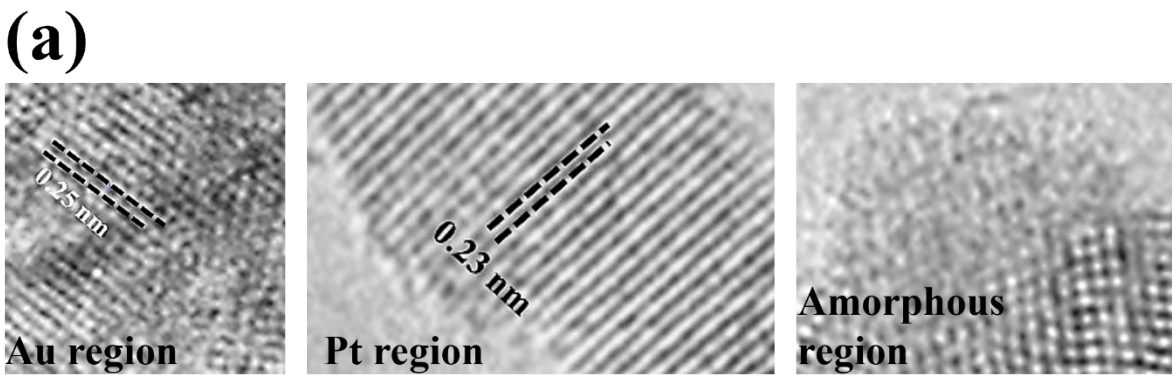

(b)

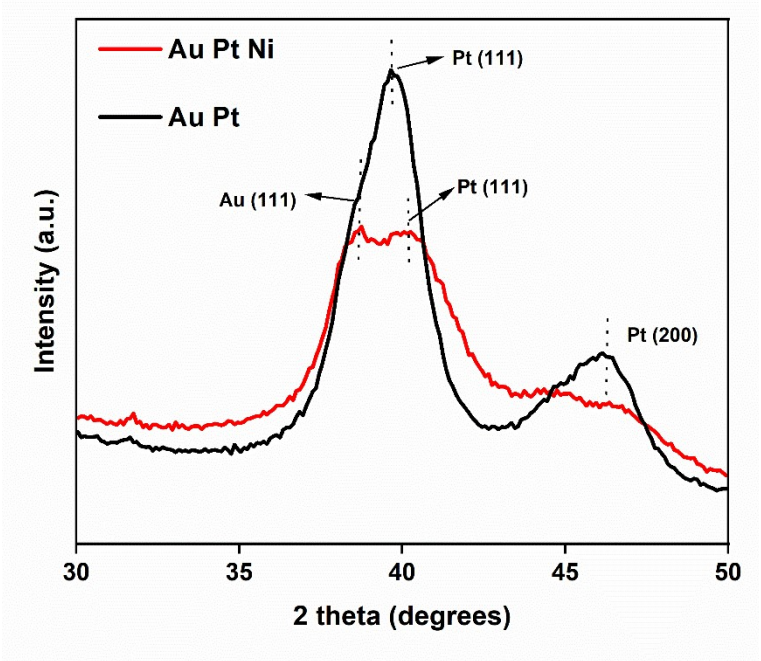


**Figure S3** (a) HRTEM images showing the lattice spacing in the Au and Pt regions and the disordered amorphous regions with no features. (b) GIXRD (Grazing Angle X-ray Diffraction) of Au-Pt-Ni bimetallic catalyst and Au-Pt catalyst.

(a)

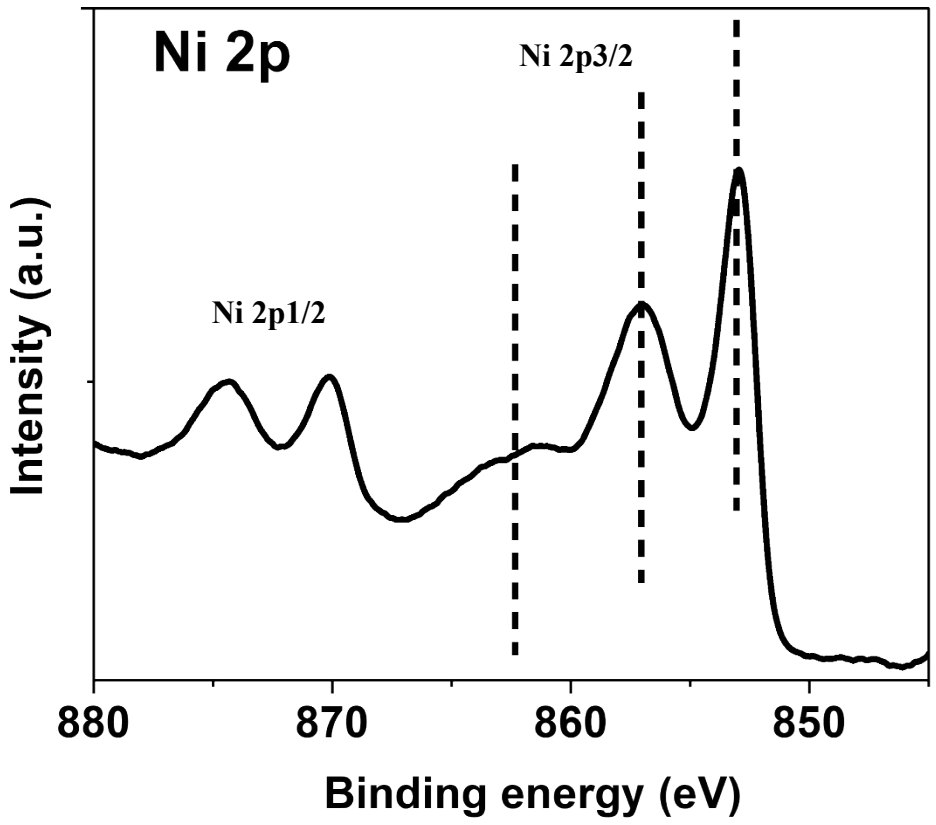

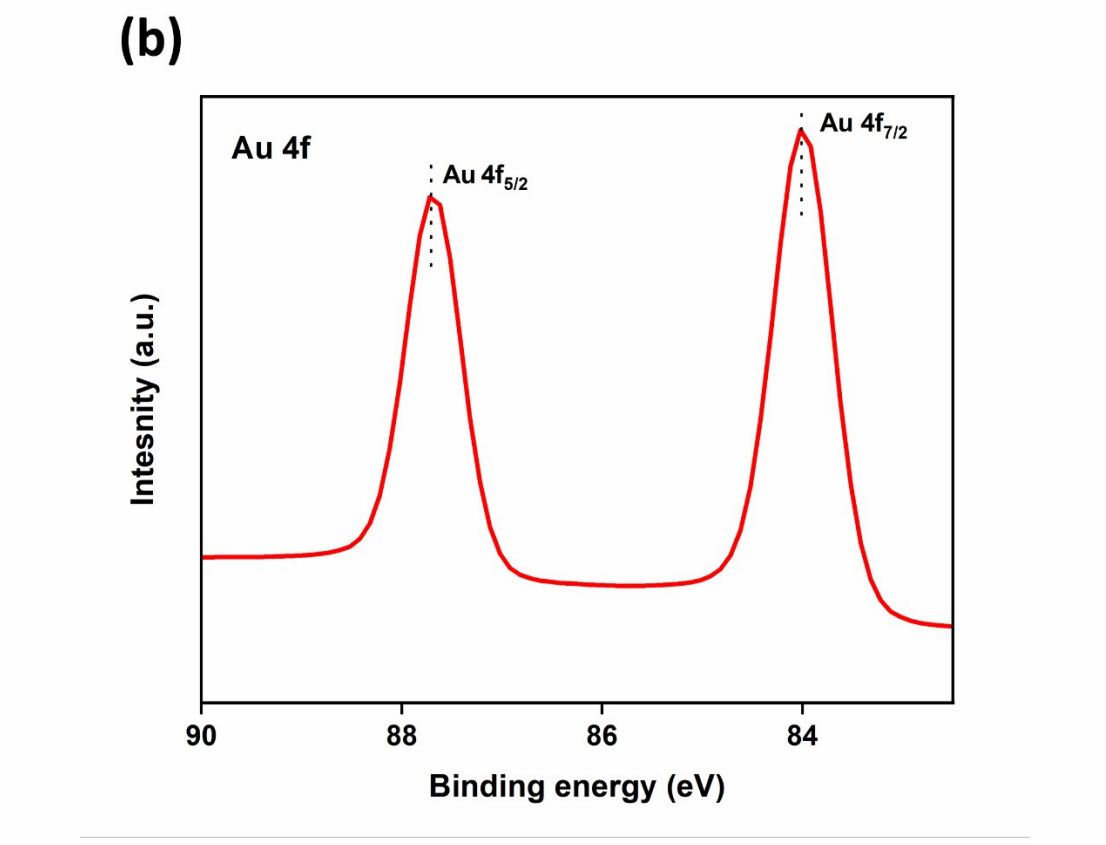


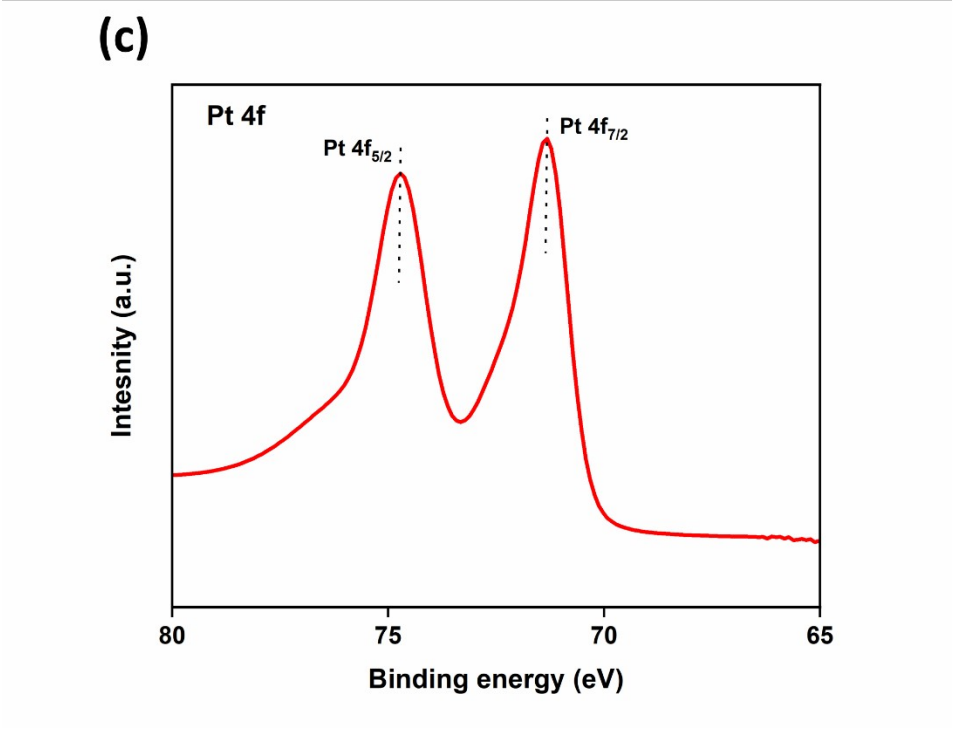


**Figure S4** XPS (X-ray Photoelectron Spectroscopy) results of Au-Pt-Ni bimetallic catalyst (a) High resolution Ni 2p XPS spectra. (b) High resolution Au 4f spectra. (c) High resolution Pt 4f spectra.

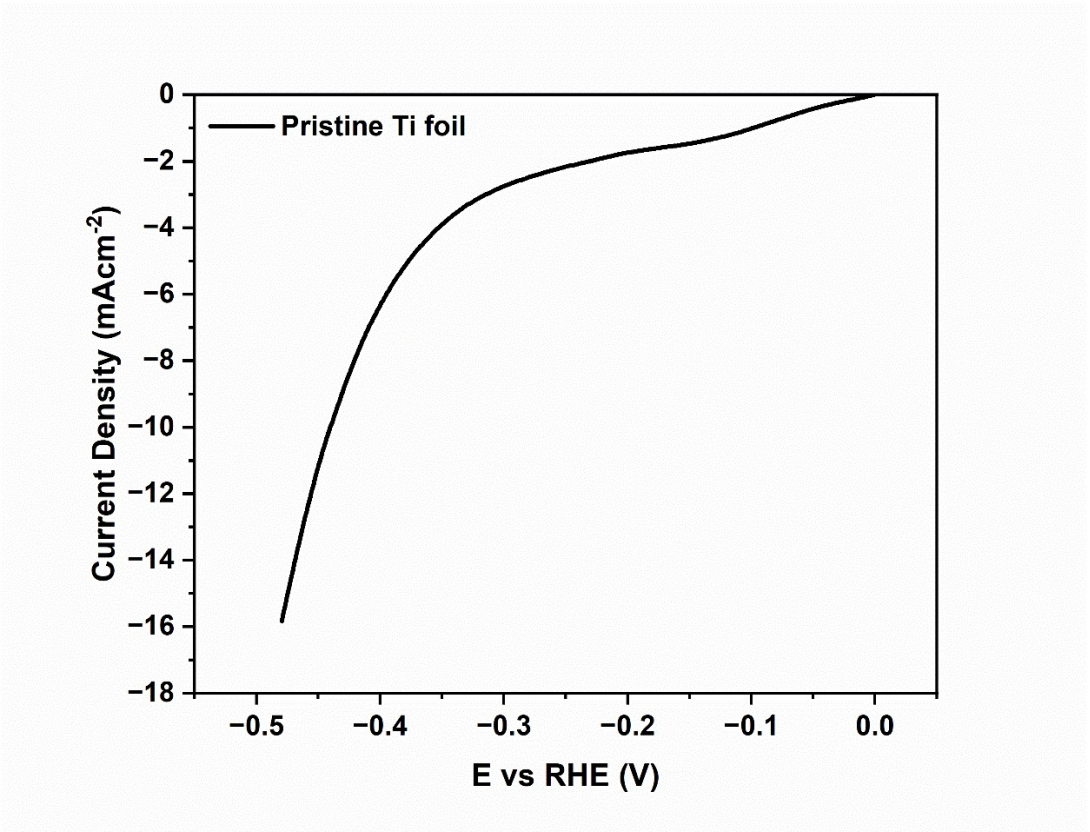


**Figure S5** LSV curve of Pristine Ti foil in 0.5 M $H_2SO_4$ solution.

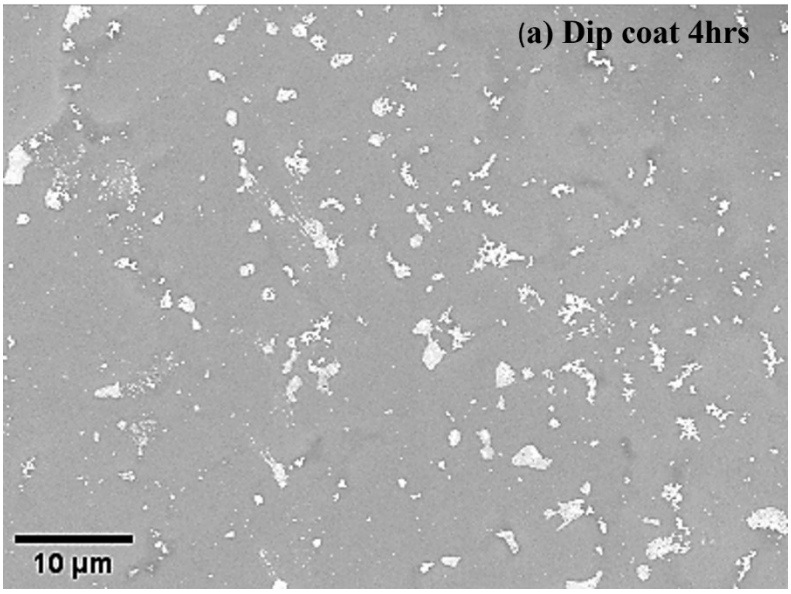

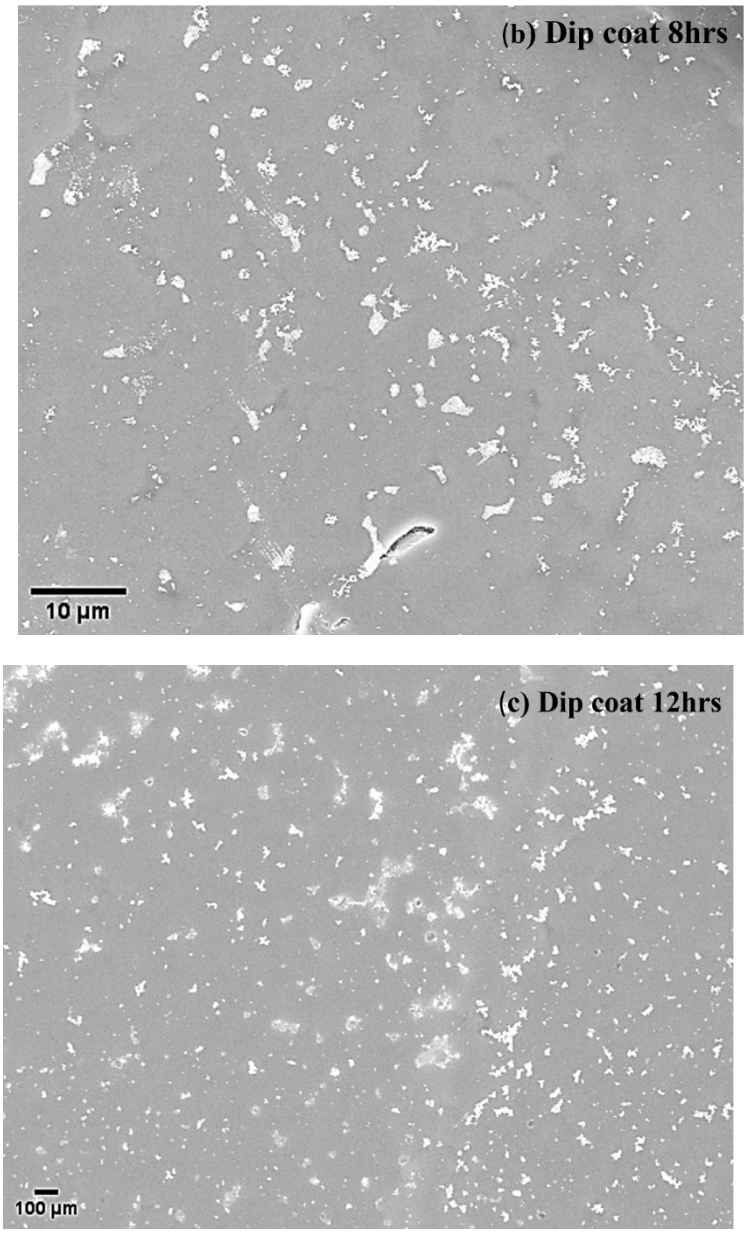


**Figure S6** (a, b & c) FESEM images of dip coated chains for various time duration showing different surface coverage.

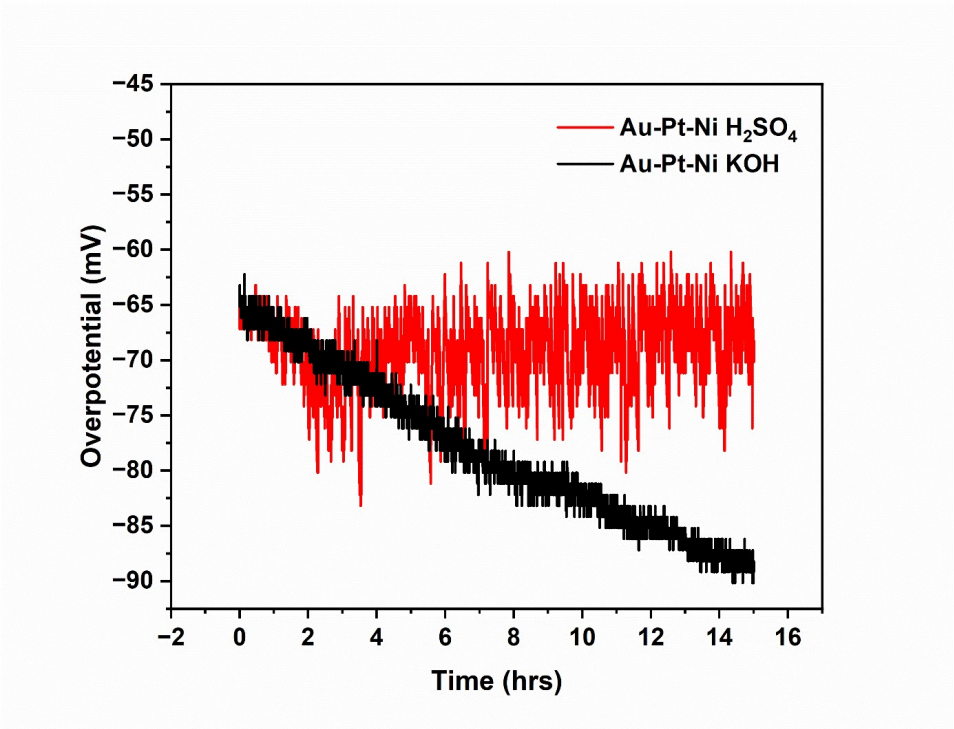


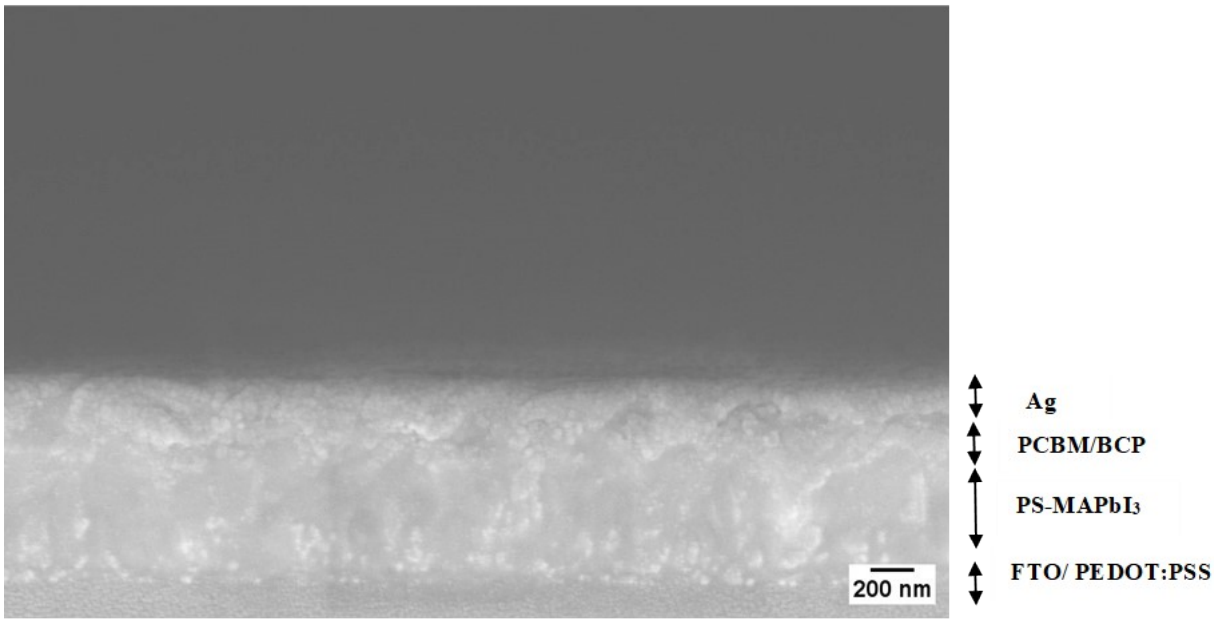


**Figure S7** Chronoamperometry scan of Au-Pt-Ni in KOH (blue) and $H_2SO_4$ (orange) for 15 hrs.

**Figure S8** Cross section SEM of PS modified solar cell showing various layers.

In the presence of moisture, the Lewis acid ($PbI_2$) hydrolyzes and results in formation of hydrogen iodide (HI). The $PbI_2$ interact with PS in the presence of HI and leads to the formation of cation complex on the main chain, i.e. polymeric cations complex with $PbI_3^-$.

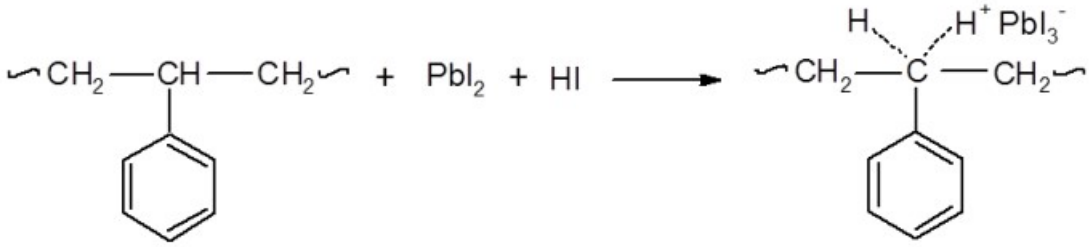

The polymeric cations complex is then converted into the carbonium ions by losing hydrogen ($H_2$), which subsequently causes cross-linking of the PS chains.

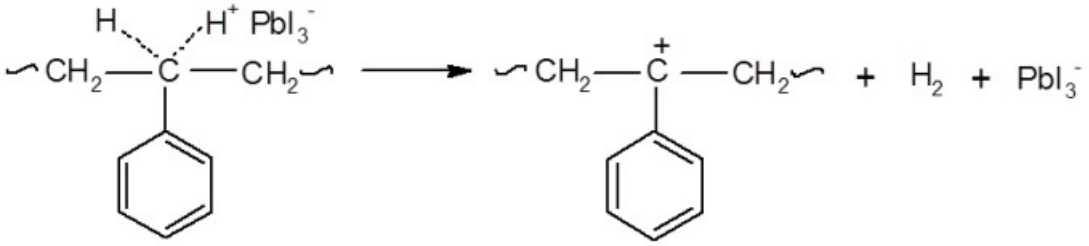

The carbonium ion on the aromatic ring then reacts with another PS chain and leads to crosslinking PS matrix in perovskite.

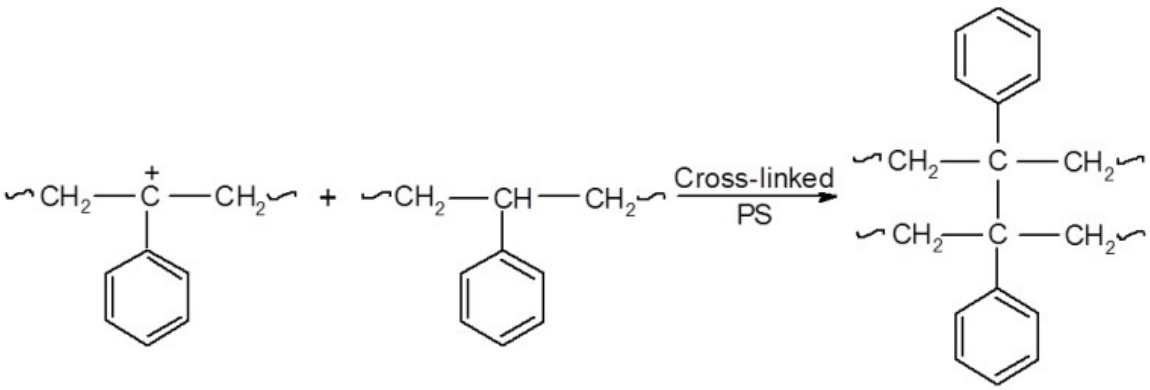


**Figure S9** Detailed PS crosslinking mechanism in the perovskite matrix.

(a)

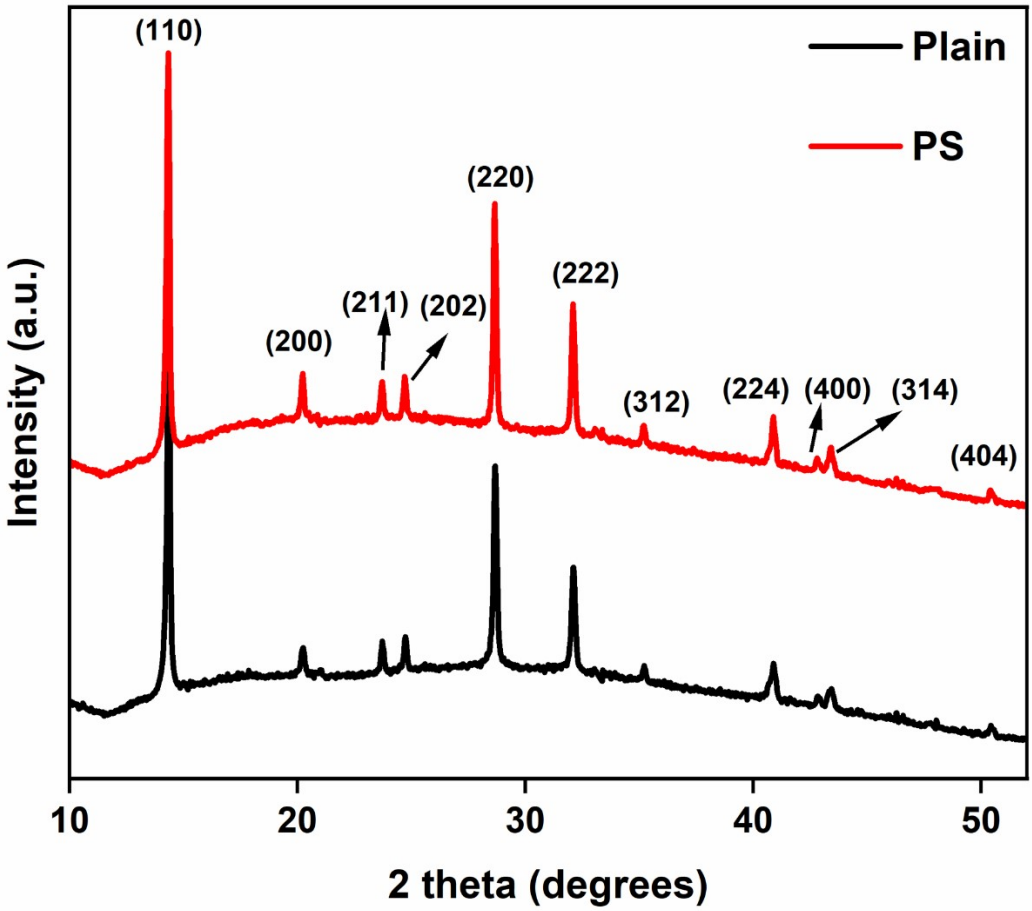
(110)
Plain
PS
(220)
(222)
(211)
(202)
(200)
(312)
(224)
(400)
(314)
(404)
Intensity (a.u.)
10
20
30
40
50
2 theta (degrees)

(b)

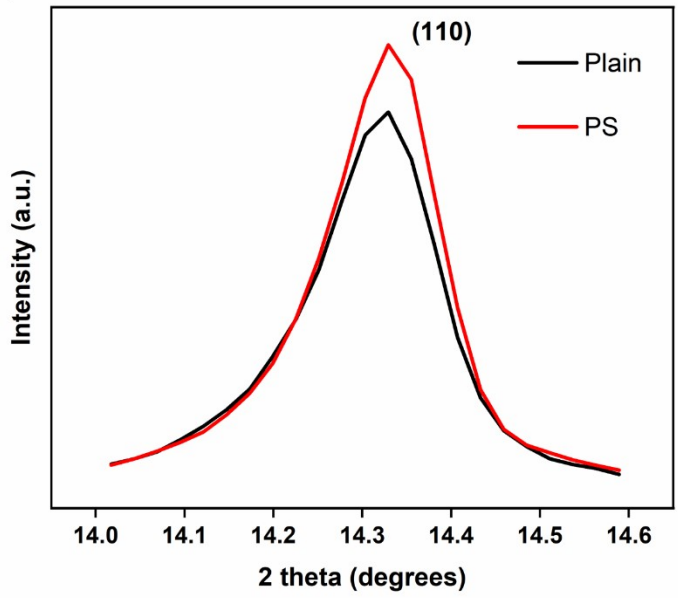
(110)
Plain
PS
Intensity (a.u.)
14.0
14.1
14.2
14.3
14.4
14.5
14.6
2 theta (degrees)

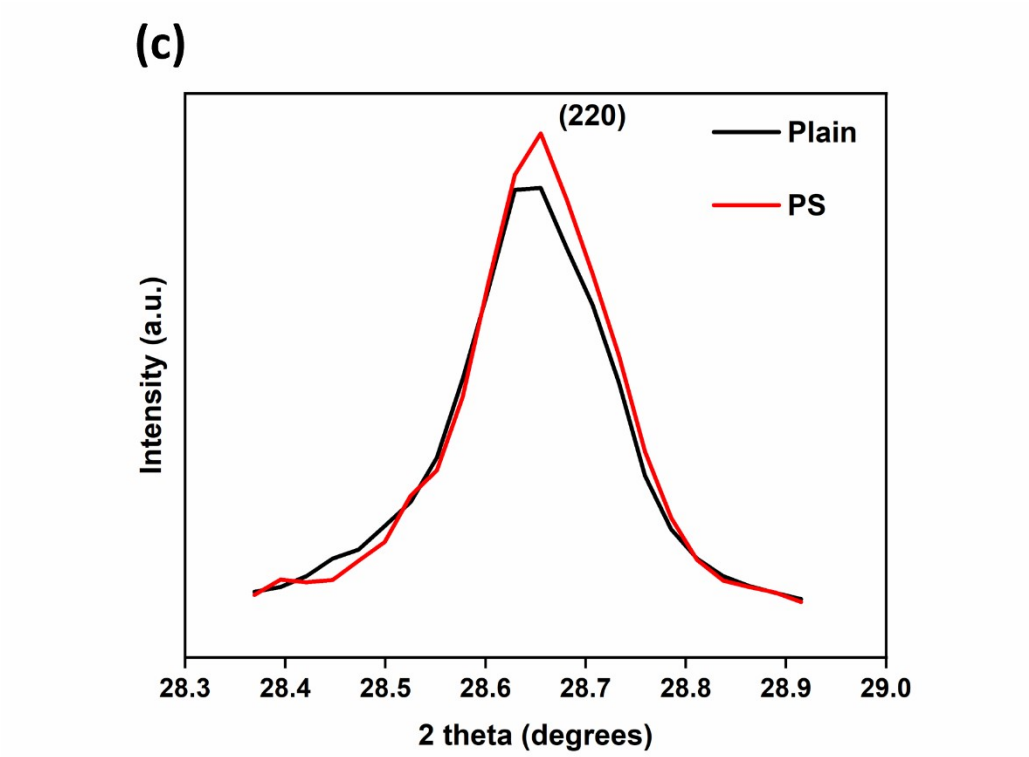


**Figure S10** (a) XRD spectra of Plain and PS $MAPbI_3$ thin films. (b, c) Zoomed in spectra of 110 and 220 peaks.

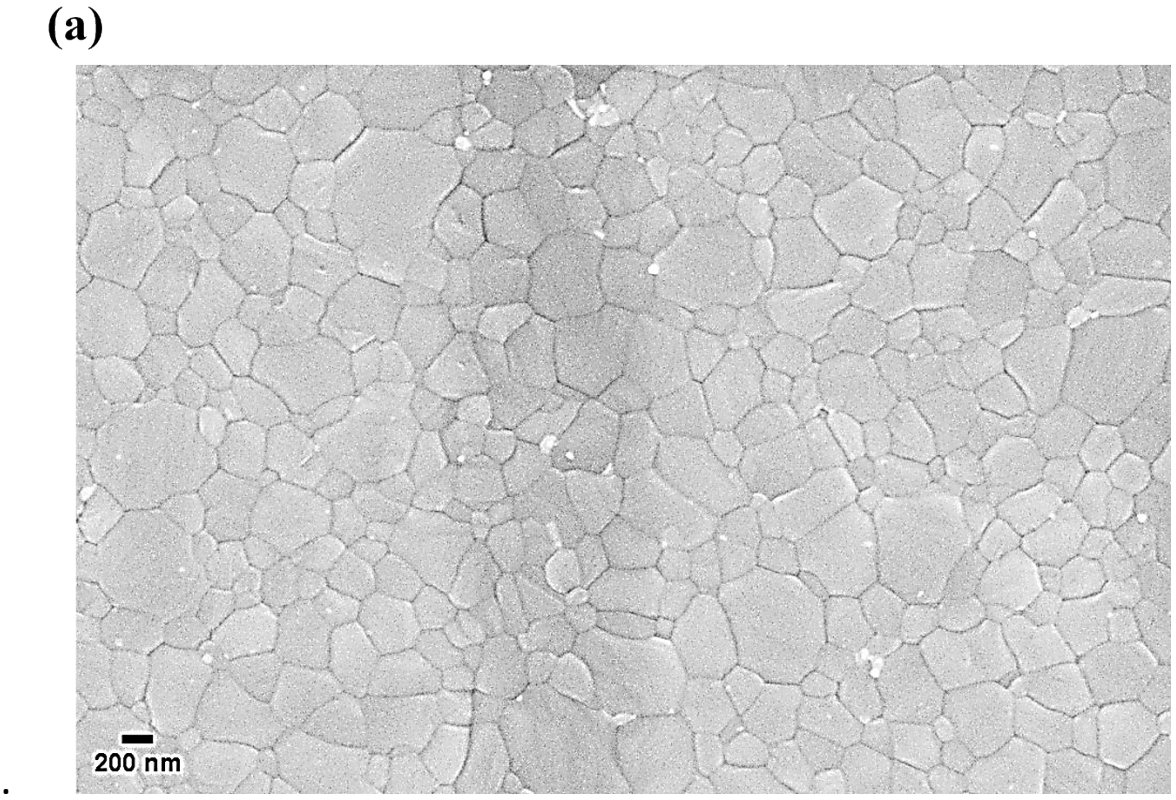


.

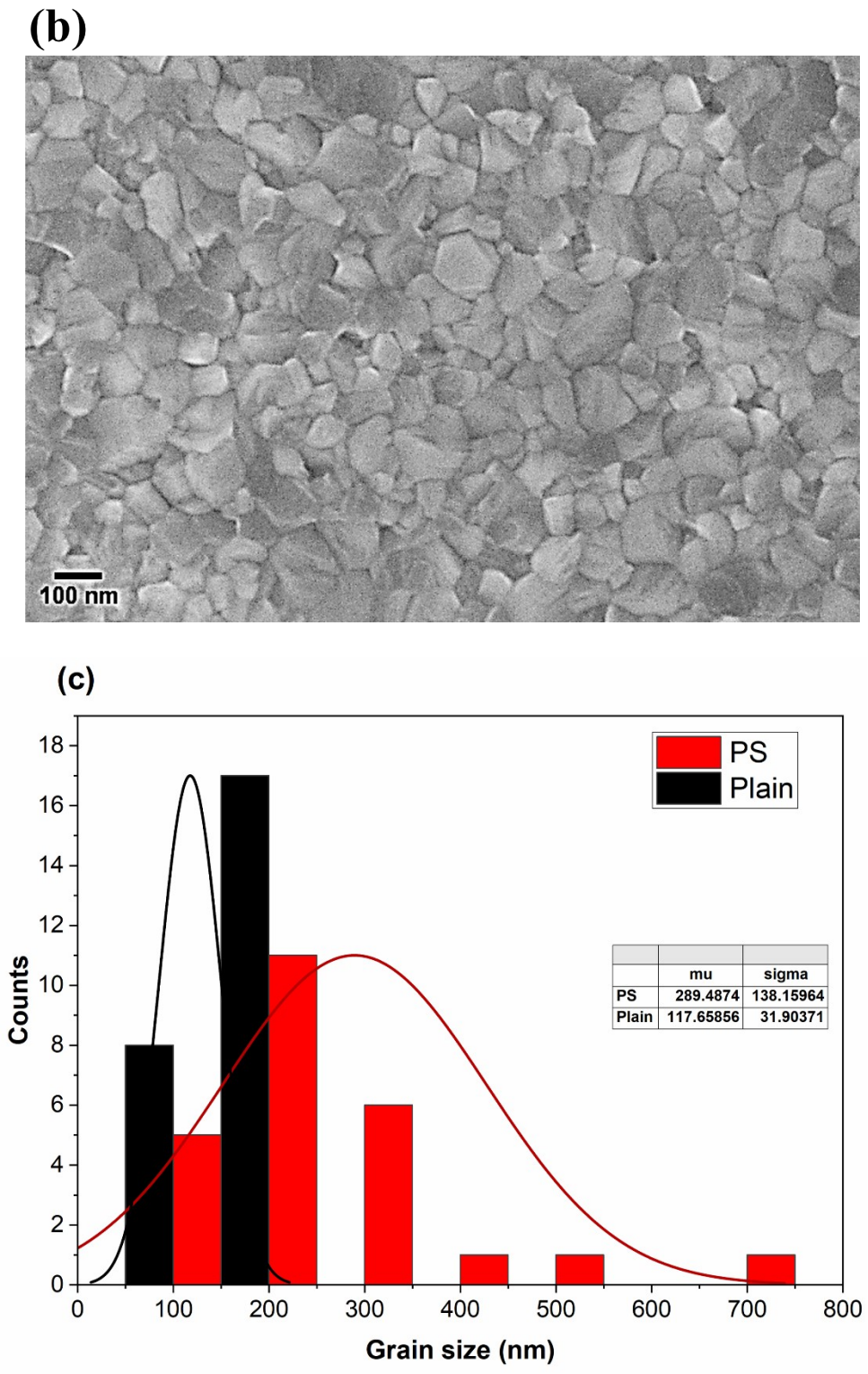


**Figure S11** (a, b) FESEM images of PS and Plain $MAPbI_3$. (c) box plot of the grain size distribution of PS and Plain samples.

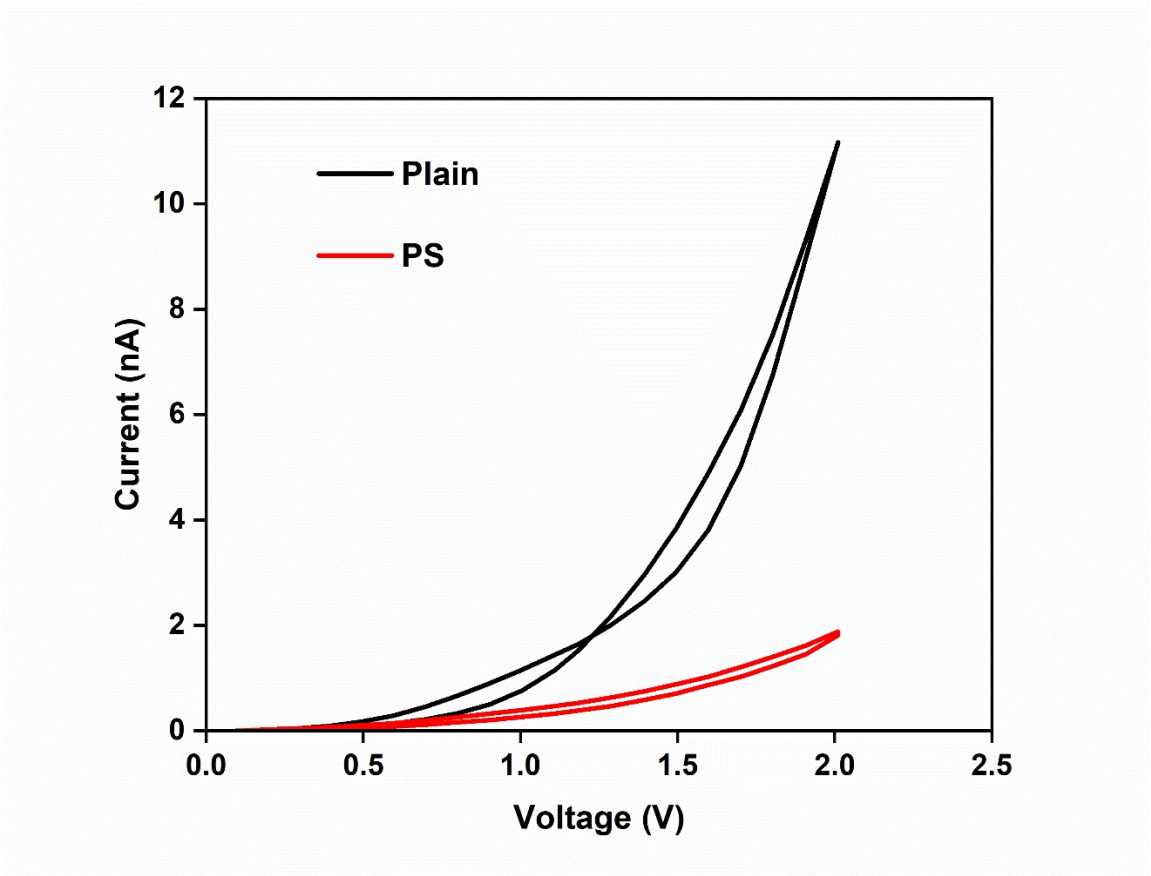


**Figure S12** showing the IV curve of PS and Plain lateral device.

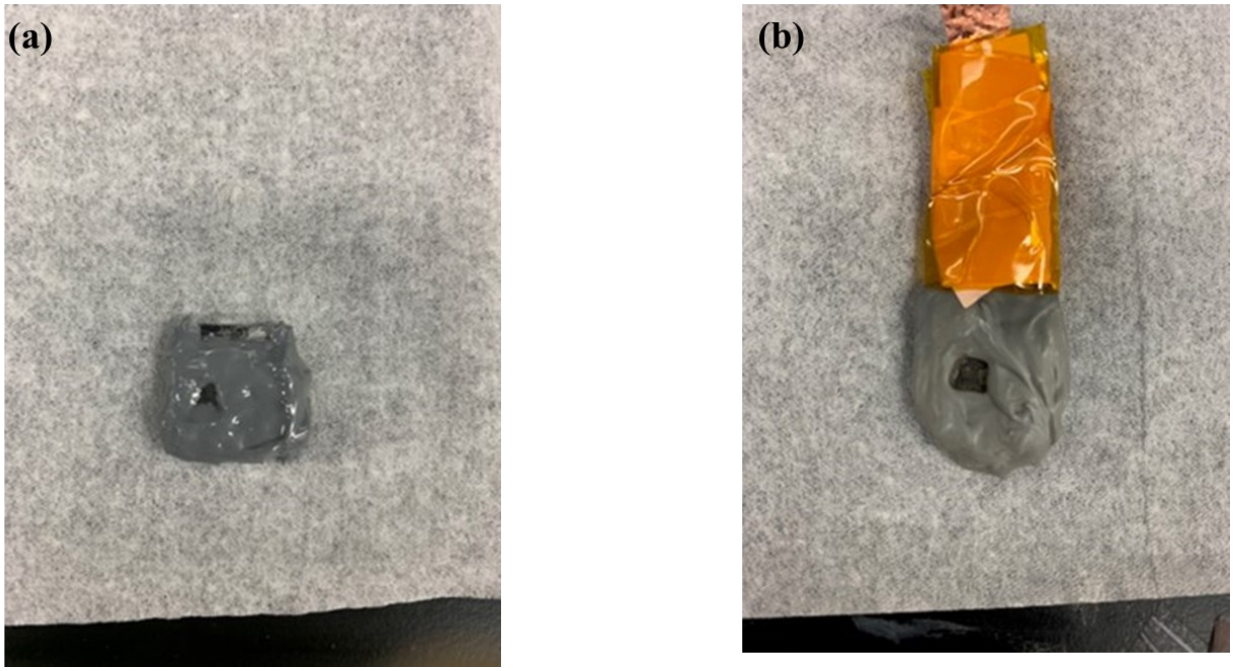


**Figure S13** (a) showing the freshly sealed photocathode with epoxy resin (b) the image of photocathode after continuous operation for 120 hrs.

**Figure S14** is the three-electrode set up of our PEC cell with simulated AM 1.5G illumination to the photocathode.

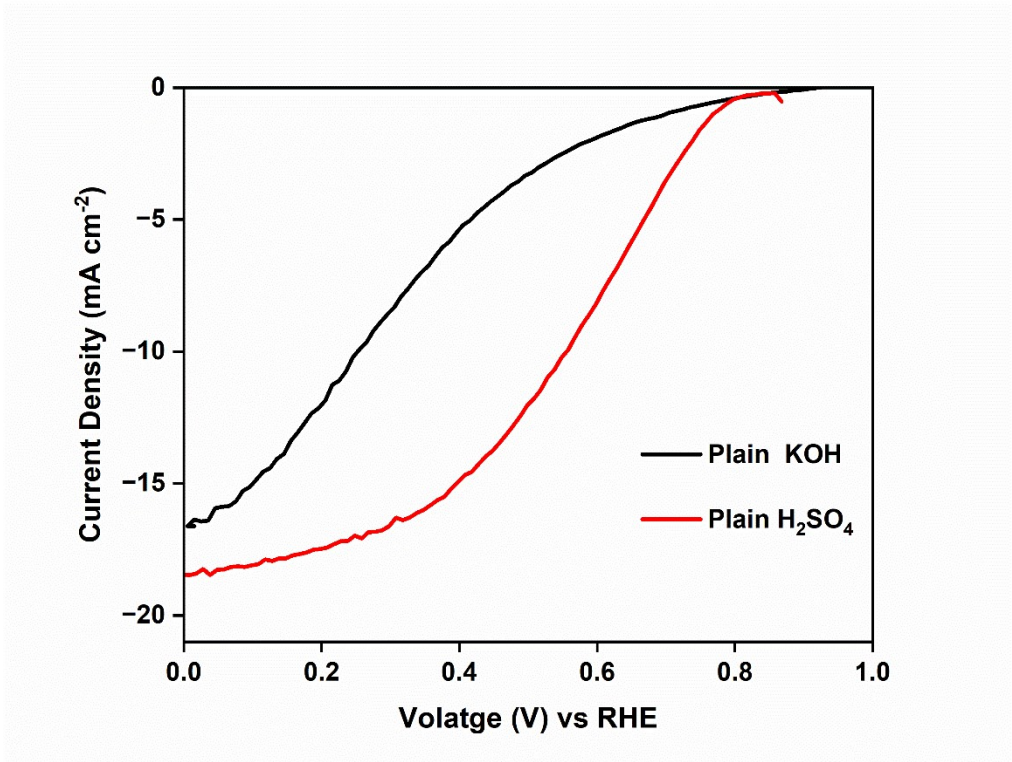


**Figure S15** showing the LSV curves of Plain $MAPbI_3$ samples in KOH and $H_2SO_4$ solution.

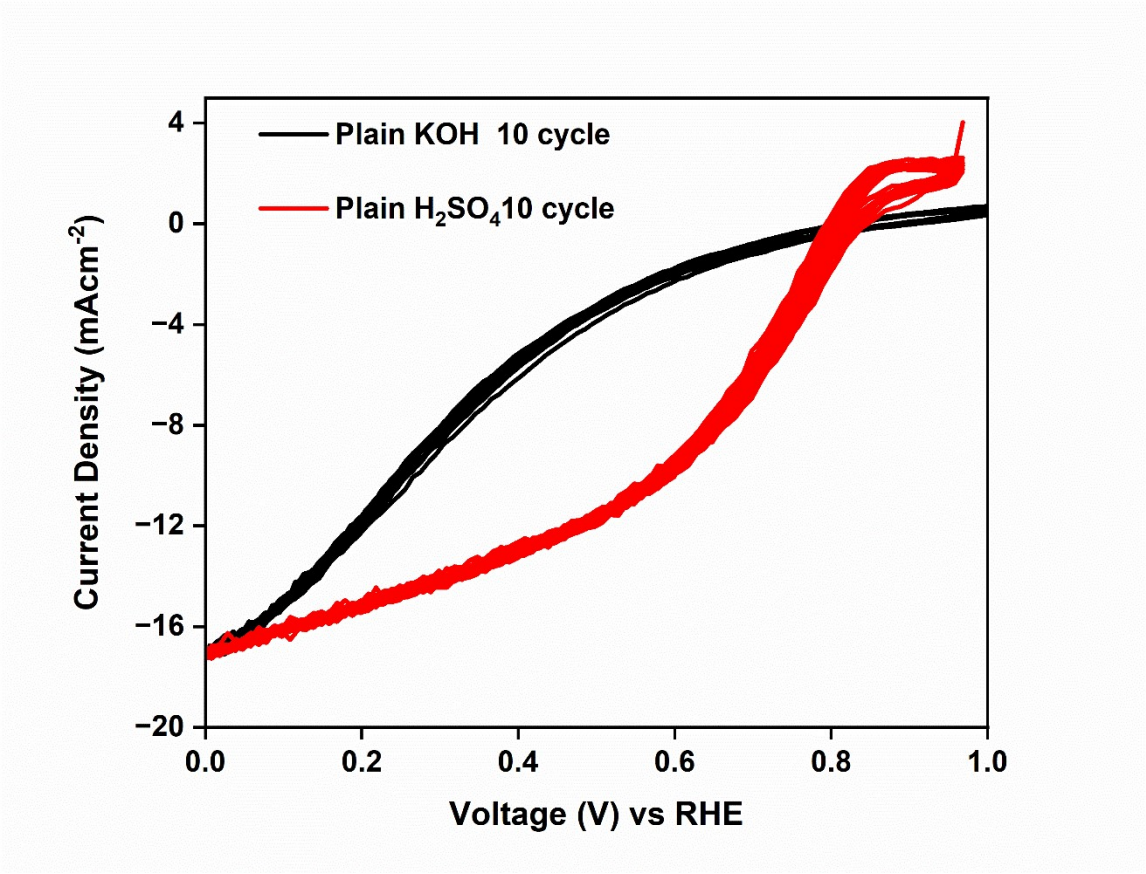


**Figure S16** showing the 10 CV cycles of plain $MAPbI_3$ in KOH and $H_2SO_4$ electrolyte conditions.

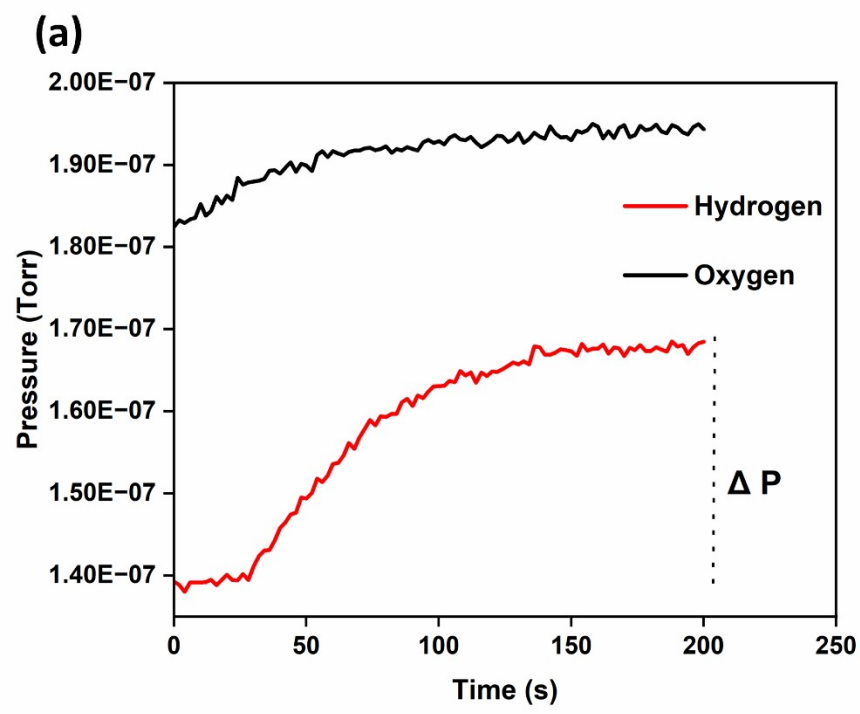

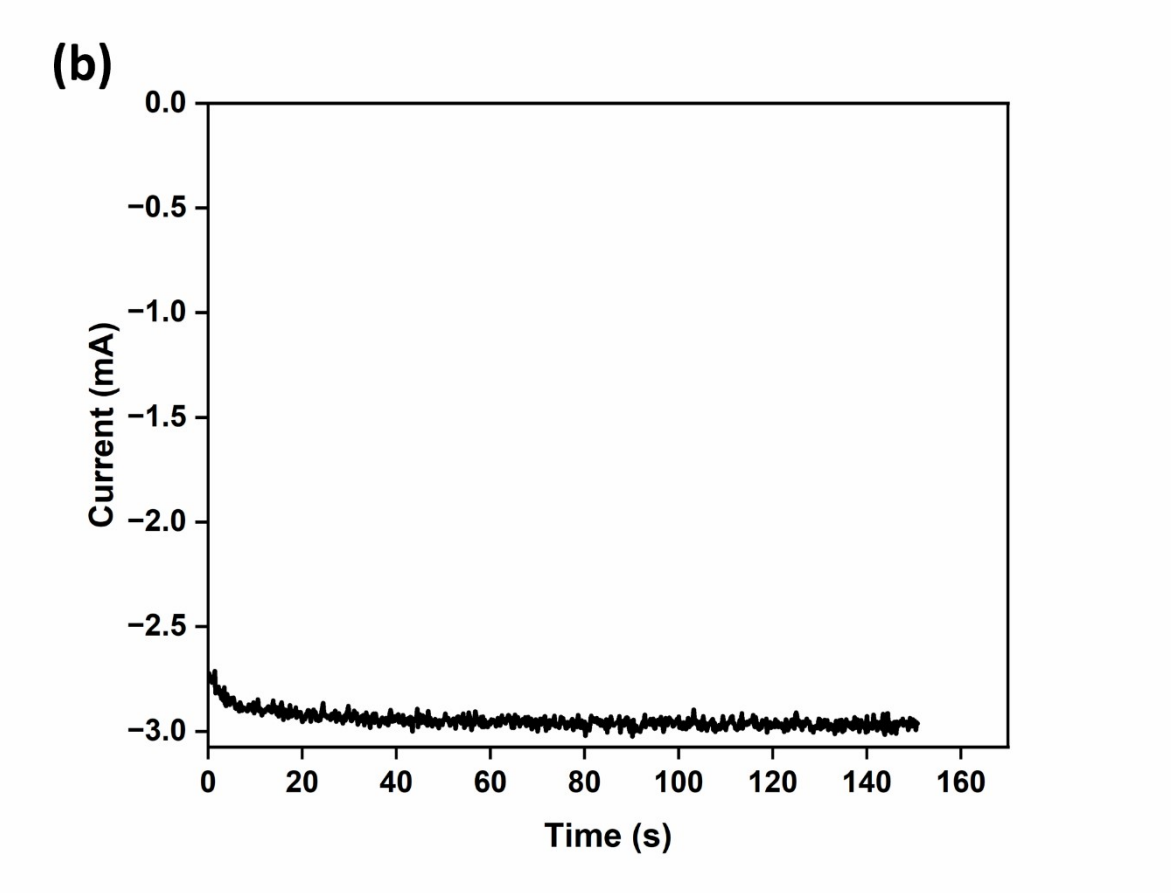


**Figure S17** a) partial pressures of $H_2$, $O_2$, before and during the HER reaction are monitored in real time. The Δ P is calculated by noting the initial and saturation pressure. b) Chronoamperometry scan showing average current of the photocathode at 0 V vs RHE, AM 1.5 G light illumination for 150s (until hydrogen saturation pressure).

**Faradaic efficiency calculation**

To quantify the evolved $H_2$ and $O_2$, gases are measured by using a Stanford Research Systems Universal Gas Analyzer system. A custom designed system using three-electrode electrochemical cell and 1.8 m long capillary tube (175 µm ID) to collect the generated gases during the reaction in a sealed quartz beaker.[1]

Pressure in the quartz beaker = 1 atm = 760 Torr

Operating pressure of the mass spectrometer = $6.45\times10^{-6}$ Torr

reduction factor = 760 Torr / $6.45\times10^{-6}$ Torr = $1.17\times10^{8}$

From Figure S Δ P after hydrogen saturation 150 s = $0.3\times10^{-7}$ Torr

Actual partial pressure of $H_2$ in the quartz beaker = P

= ($0.3\times10^{-7}$ Torr) × ($1.17\times10^{8}$) = 3.51 Torr = 467.96 Pa

Volume of space above the liquid in the beaker = total hydrogen volume = V = $1.2\times10^{-5}$ $m^3$

Number of moles of $H_2$ generated after 150 s of reaction = n = PV/(RT)

= (467.96Pa) ($1.2\times10^{-5}$ $m^3$) / [(8.314 Pa $m^3$ K $mol^{-1}$) (298 K)] = $0.22\times10^{-5}$ mol

To produce 1 molecule of $H_2$ it needs 2 electrons based on the reaction ($2H_2O + 2e^- \rightarrow H_2 + 2OH^-$), so the total number of electrons required for HER during 150 s per sample area is calculated by:

N(e-gas) = n*2*6.023E23 $mol^{-1}$ ; N(e-gas) = $0.265\times10^{19}$ electrons

Total number of electrons generated over 150 s is given by average current in Figure S13b :

N(e-current) = I*t/1.60E-19 C

= ($2.92\times10^{-3}$ A) (150 s) / ($1.60\times10^{-19}$ C) = $0.273\times10^{19}$ electrons

where t the chronoamperometry program time program running time (150 s). Finally, Faradaic efficiency is expressed by:

FE = N(e-gas)/N(e-current)*100% = 97.06%

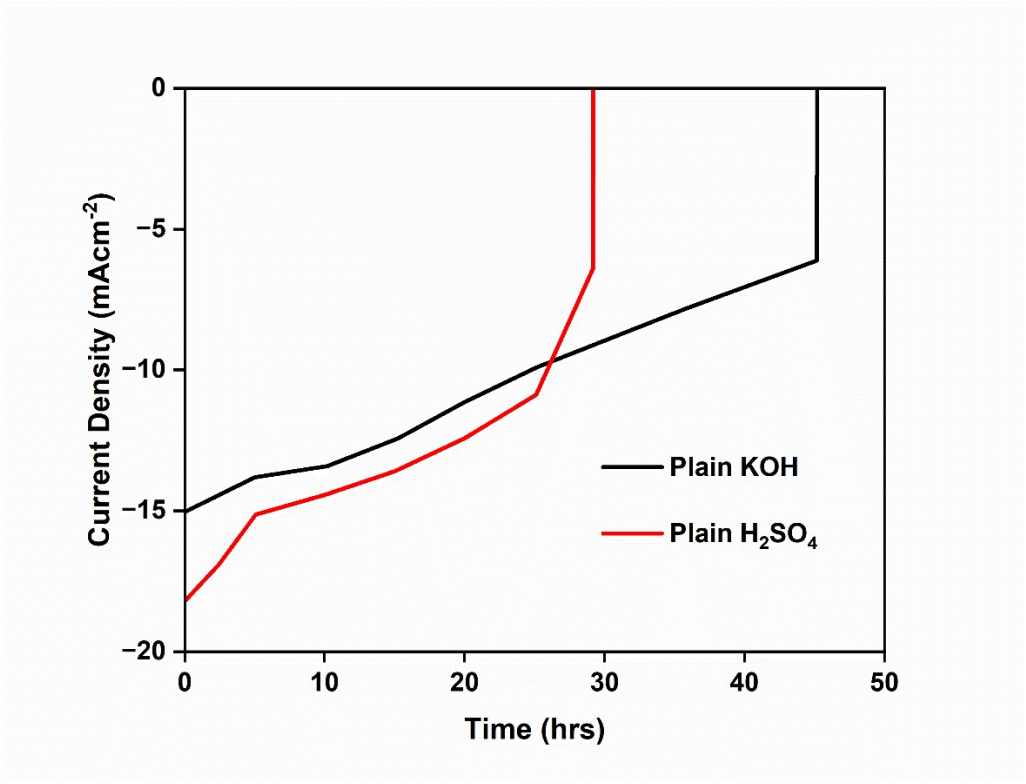


**Figure S18** showing chronoamperometry scan for plain devices in KOH and $H_2SO_4$ solutions.

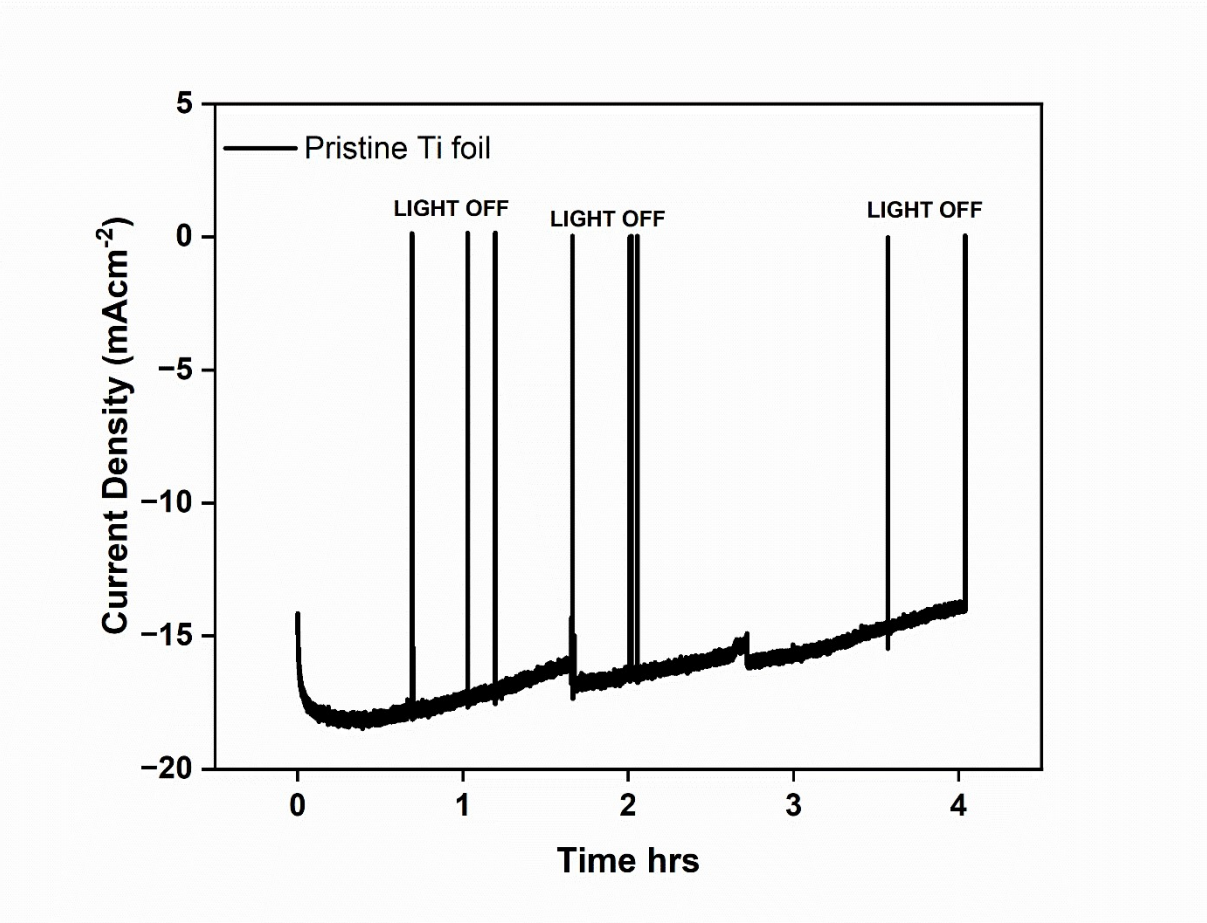


**Figure S19** showing chronoamperometry scan for pristine Ti foil in $H_2SO_4$ solution.

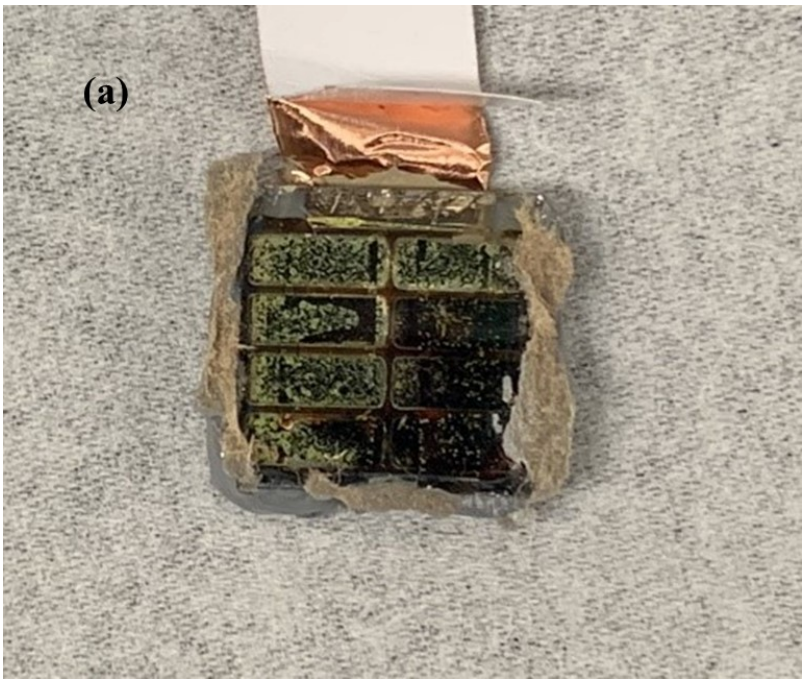

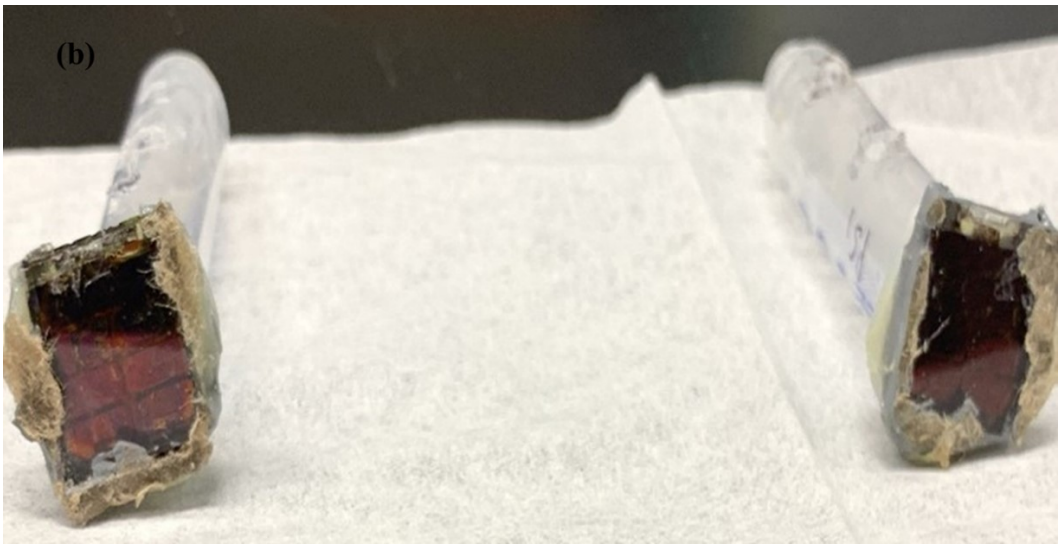


**Figure S20** (a) showing the yellow color spots and discoloration seen in plain photocathode. (b) showing negligible discoloration after 120 hrs. continuous operation of PS based photocathode.

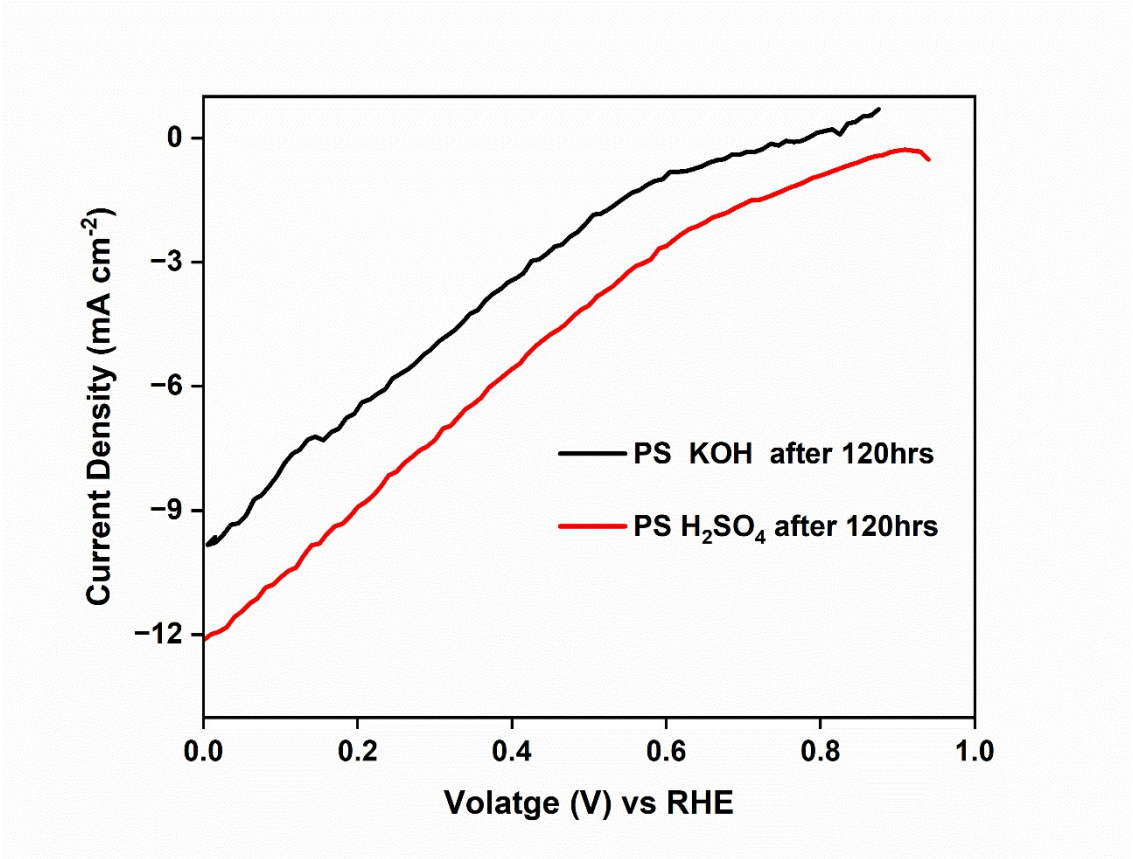


**Figure S21** showing the LSV curves of PS device after 120 hrs. operation in $H_2SO_4$ and KOH solution.

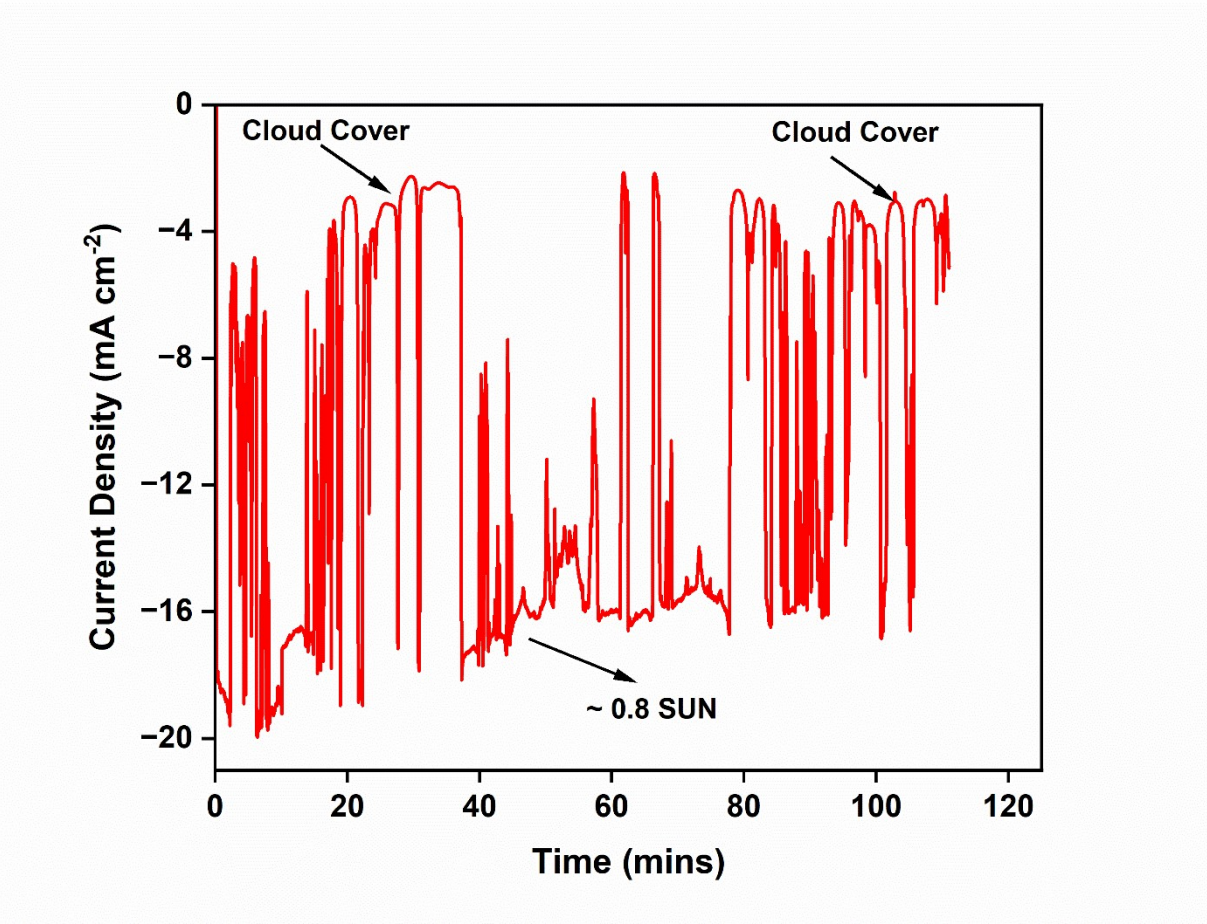


**Figure S22** showing chronoamperometry scan (at 0 V vs RHE) of PS based photocathode in natural sunlight. The fluctuations in current are due to changes in light intensity from varying cloud cover.

**Table S23** Comparison of the PCE device with other reports in literature.

| **Photocathode** | **Catalyst** | **$J_{ph}$ at 0V vs RHE ($mA.cm^{-2}$)** | **$E_{onset}$ (V vs RHE)** | **Stability ($T_{80}$)** | **Electrolyte** | **Reference** |
|---|---|---|---|---|---|---|
| **PS- $MAPbI_3$** | Au-Pt-Ni nanochains | -20.03 | 0.95 | 78 hrs (KOH) 70 hrs ($H_2SO_4$) | 0.5 M $H_2SO_4$ and 0.5M KOH | This work |
| **$MAPbI_3$ with proline** | Pt np | -21.7 | 1.1 | 17.5 hrs | 0.5M $H_2SO_4$ | 2 |
| **$MAPbI_3$** | Pt np | -9.8 | 0.95 | 1.7hrs | 0.1M borate | 3 |
| **$MAPbI_3$** | Pt np | -18.1 | 0.95 | 4.5hrs | 0.5M $H_2SO_4$ | 4 |
| **$MAPbI_3$ with proline** | $MoS_2$ | -20.6 | 1.02 | 40.7 hrs | 0.M $H_2SO_4$ | 5 |
| **$CsPbBr_3$** | Pt np | -1.2 | 1.16 | 3.5 hrs | 0.2M/ L $Na_2HPO_4$/ $NaH_2PO_4$ | 6 |
| **CsMAFA perovskite** | Pt np | -10.5 | 0.68 | 1.7hrs | 0.5M $H_2SO_4$ | 7 |
| **CsMAFA perovskite** | Pt np | -12.1 | 0.6 | 4.5hrs | 0.1M KOH (with 0.1M $K_2So_4$) | 8 |

**Table S24** Inductively Coupled Plasma Optical Emission spectroscopy (ICP-OES) elemental analysis of the electrolyte before and after long term stability testing.

| Sample ID | Line/ Element | Reporting limit (RL) (mg/L) | Concentration (mg/L) |
|---|---|---|---|
| Electrolyte Before | Au 242.795 r | 0.1 | < RL |
| Electrolyte After Long term Chronoamperometry | Au 242.795 r | 0.1 | < RL |
| Electrolyte Before | Pt 214.423 r | 0.1 | < RL |
| Electrolyte Before | Pt 265.945 r | 0.1 | < RL |
| Electrolyte After Long term Chronoamperometry | Pt 214.423 r | 0.1 | < RL |
| Electrolyte Before | Ni 221.648 r | 0.05 | < RL |
| Electrolyte After Long term Chronoamperometry | Ni 221.648 r | 0.05 | < RL |
| Electrolyte Before | Pb 220.353 r | 0.2 | 3.4 |
| Electrolyte After Long term Chronoamperometry | Pb 220.353 r | 0.2 | 3.6 |

The Pb in the electrolyte can be due to the residual heavy elements in the acidic medium, $H_2SO_4$.

# References


1 A. Rahman, J. P. Thomas, K. T. Leung, M. A. Rahman, J. P. Thomas and K. T. Leung, *Adv. Energy. Mater.*, 2018, **8**, 1701234.

2 J.-H. Kim, S. Seo, J.-H. Lee, H. Choi, S. Kim, G. Piao, Y. Ryun Kim, B. Park, J. Lee, Y. Jung, H. Park, S. Lee, K. Lee, J. Kim, S. Seo, H. Choi, S. Kim, J. Lee, Y. Jung, S. Lee, K. Lee, B. Park, J. Lee, G. Piao, H. Park and Y. R. Kim, *Adv. Funct. Mater.*, 2021, **31**, 2008277.

3 M. Crespo-Quesada, L. M. Pazos-Outón, J. Warnan, M. F. Kuehnel, R. H. Friend and E. Reisner, *Nat.Commun.* , 2016, **7**, 1–7.

4 H. Zhang, Z. Yang, W. Yu, H. Wang, W. Ma, X. Zong and C. Li, *Adv. Energy. Mater.* , 2018, **8**, 1800795.

5 H. Choi, S. Seo, J. H. Kim, J. H. Lee, S. Kim, G. Piao, H. Park, K. Lee and S. Lee, *J .Mater. Chem. A* , 2021, **9**, 22291–22300.

6 L.-F. Gao, W.-J. Luo, Y.-F. Yao, Z.-G. Zou, R. Li, Chem comm, 2018, **54**, 11459–11462.

7 I. S. Kim, M. J. Pellin and A. B. F. Martinson, *ACS Energy Lett.*, 2019, **4**, 293–298.

8 V. Andrei, R. L. Z. Hoye, M. Crespo-Quesada, M. Bajada, S. Ahmad, M. De Volder, R. Friend and E. Reisner, *Adv. Energy. Mater.*, 2018, **8**, 1801403.